Design, manufacture, and testing of customized sterilizable respirator

Ruohan Xu [a,b,c], Libin Yang [a,b], Zhao Qin [a,b,d,*]

[a] Laboratory for Multiscale Material Modeling, Syracuse University, 151L Link Hall, Syracuse, NY, 13244, USA
[b] Department of Civil and Environmental Engineering, Syracuse University, 151L Link Hall, Syracuse, NY, 13244, USA
[c] Department of Mechanical and Aerospace Engineering, Syracuse University, 151L Link Hall, Syracuse, NY, 13244, USA
[d] The BioInspired Institute, Syracuse University, NY, 13244, USA

ABSTRACT

The respirator as one of the personal protective equipment is essential for industrial activities (e.g., mining, painting, woodcutting, manufacturing) for protection from contaminants in the air and during the Covid-19 pandemic to protect the wearer from infection. The respirators nowadays are commonly made of rigid plastic. They are expensive, cumbersome, and not comfortable to wear. The many components with complex structures prevent it from cleaning and reusing. We develop a practical and scalable strategy to create customized respirators with durability using computational modeling and 3D printing. It is shown that by morphing the shape according to the user's photo, the respirator is designed to fit a user's face without air leaks. Using a printing-mold-casting method, this respirator can be manufactured by silicone rubber with accuracy, which is highly durable, with its mechanics primarily not affected by sterilization. These features provide the current respirator adaptivity and convenience in carrying and storing, as well as more comfort for long-time wearing.

1. Introduction

Due to the worldwide outbreak of COVID-19, the shortage of medical masks has always been a problem worldwide. At this stage, most medical masks are disposable after a single usage. According to the World Health Organization (WHO) modeling (Chaib, 2020), an estimated 89 million medical masks are required for the COVID-19 response each month as this crisis is likely to persist for some time, and people need daily consumption for personal protection (Xiang et al., 2020). The practical filtering part of most face masks are manufactured with melt-blown non-woven fabric, and their manufacturing requires either polypropylene or polyethylene, polyurethane, polystyrene, polycarbonate, polyacrylonitrile as the raw materials (Akber Abbasi et al., 2020). The production process also needs high energy input for material melting and fiber spinning and heavy machines for massive production (Rubio-Romero et al., 2020). Moreover, ecological concern has resulted in the urge to limit the use of polypropylene, as it takes more than 10 years to decompose in landfills completely and only 7 percent of such waste is currently used for post-consumer recovery (Canopoli et al., 2020; Oladimeji Azeez, 2020). The ongoing global-wide COVID-19 disease significantly affects the everyday routine of human life as the respirator becomes primary personal protective equipment. Massive

usage of the single-use disposable mask causes long-term environmental issues. There is currently no effective way to collect, isolate and recycle them. Using the respirators that can be re-sterilized can significantly reduce the amount of waste and make the filter material exchangeable, making it also possible to collect and recycle the filter material over time.

A sterilizable mask is desirable to reduce the need of melt-blown non-woven fabric materials (Chellamani et al., 2013). A conventional surgical mask turns out to be effective for personal protection because it covers the face to protect the nose and mouth from exposure to splashes, sprays, splatter, and respiratory secretions (Chellamani et al., 2013). It is also helpful for source control in the public area as it prevents the spread of respiratory secretions when sick people are talking, sneezing, or coughing. The currently FDA-cleared masks are made of a universal shape for averaged face profile and sometimes may fail to close contact with an individual face. One recent study shows that a low-cost 3D-printed frame significantly improves its inward protection efficiency for airborne particles known to transmit COVID by pushing against the face and establishing a form-fitting seal, which improves the efficiency in protection by effectively turning the flat cloth mask into a well fitted one (Tong et al., 2021). It is innovative as the 3D model is highly customized according to the face profile, while it is necessary to

---

use a large piece of cloth to cover the most area of the face.

A respirator is a device designed to protect the wearer from inhaling dangerous air, including particulate matter such as dust and airborne microorganisms, as well as harmful fumes, vapors, and gases. It is widely used in medical, industrial, construction, etc. All respirators can be secured to the wearer's head by straps that generate compression between the wearer's face and the device. The respirator covers the entire face or the lower part of the face, including the nose and mouth. There are many different styles and sizes to suit all face shapes. The difference in the design of the respirator will affect the protection coefficient assigned by the respirator, that is, what kind of hazard the level of protection produced. According to the Center for Disease Control and Prevention (CDC), three filter efficiency N, R, and P (95%, 99%, and 99.97%) are commonly used in the design of the respirator (NIOSH, 1996). If worn correctly, the filtering capacity of the respirator is better than that of ordinary masks and medical masks. However, even if it is worn in full compliance with the requirements, it cannot be 100% isolated from the inhalation of particles in the air. A respirator that suits the wearer's face is crucial to fits tightly and provide comfort in long-time wearing, protecting the wearer from exposure. At present, most of the respirators on the market are of universal size, but because each person's facial features are different, a universal size may not provide greatest protection. Moreover, they are made of hard plastic with a cumbersome size, making it hard to carry and store. It is assembled from multiple parts, leading to many gaps and corners that are hard to clean for reused. Once a respirator cannot be reused, it generates more waste materials than the disposable masks and they are harder to degrade (Akber Abbasi et al., 2020). Therefore, we are motivated to design innovative respirators. Our experiment focuses on reducing the size and increasing the reliability through computer modeling and analysis of facial images for customized fitting, as well as the disinfection and durability for repeating usage.

2. Materials and methods

2.1. Overall design

We combine computational modeling, 3D printing and various of experimental tests to facilitate the design of this fully customized respirator with flexibility. The overall design workflow is summarized in Fig. 1a, with each experimental method described in the following sections.

2.2. Airtight testing of the respirator

We built our platform to detect the airtightness of the respirator by measuring the CO_2 concentration. As inhalation can generate pressure less than the atmosphere and the respirator is pushed against the face, exhalation may open the gap between the respirator and face to enter unwanted airborne particles. Since the exhaled air contained a much higher concentration of CO_2 than that of air (409 ppm, 25 °C), by measuring it at the periphery of the respirator using usage (Fig. 1c), we can locate the gaps, this platform is composed of a CO_2 sensor (Analog Infrared CO_2 Sensor For Arduino by DFRobot that can sense CO_2 level between 0–5000 ppm and send a corresponding electric signal) that is connected to an Arduino board, which is used to read the electric signal from the CO_2 sensor with a scanning rate of 9600 Hz. The connection between the CO_2 sensor and Arduino board is same as any standard sensor, as illustrated in Fig. 1d, and we tried our best to ensure the connection between the sensor and Arduino board tight. The Arduino board is connected to a computer through a USB port, and Arduino IDE regulates the voltage signal from the CO_2 sensor and record the CO_2 level as a function of time (Fig. 1e). Since the respirator is made of soft material, we tested multiple places at the respirator periphery. We found that the respirator's left, right, and underside easily fit the experimenter's face by tightening the elastic stripe, which is consistent with
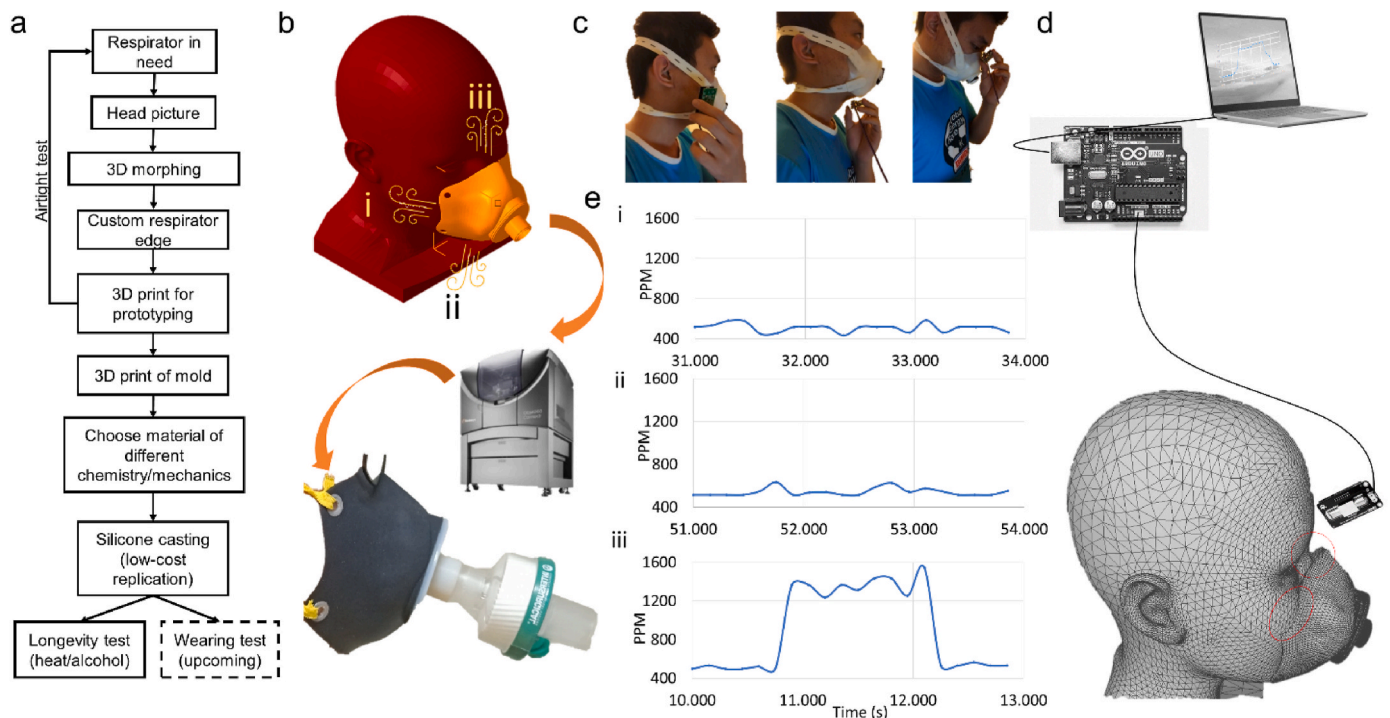
Fig. 1. **3D modeling and printing of an arbitrary respirator connecting to respiratory devices and test airtight with a CO_2 sensor. a.** schematic diagram for the design procedure of the respirator. **b.** the computational model of the respirator, the multi-material 3D printer, and the 3D printed respirator connecting to a respiratory device. **c.** The test of CO_2 of the printed mask at different positions along its edge against the face during normal breathing, **d.** schematics of how the sensor is connected to the analog input of an Arduino board and a computer, as well as the main reason for the air leak at the top of the mask. **e.** The CO_2 test results of i) at the right side, ii) at the bottom, and iii) at the top of the mask, as illustrated in panel b.

our expectations. The upper part of the respirator leaks gas and can only stop by adding a metal strip seal or changing the shape. This is like most commercial respirators have done. Once we test the respirator with both stripe and filter, the people can easily breathe without resistance.

2.3. The morphing of face profile with Blender

We used the Blender package (2.8.2) to create the human head model to reflect the customized face profile. We used the function KeenTools FaceBuilder for Blender (Version 2.1.0) to help build 3D models of head models using a couple of photographs that can be in any dimension. This is an add-on tool to BlenderApp. The FaceBuilder has a feature to capture the face shape by adding specific points, which the user needs to add the points for eyes, forehead, mouth, nose, etc. The function helps us to create a head model from a set of 2D images (at least one photo from the front and one from the side) to a 3D model that provides quick operation for the experiment. The information helps the tool determine the 3D position of the featuring points (eyes, forehead, mouth, nose, etc.) and after that alter the overall shape of the model face to maximize the match to the location of the featuring points and thus generate the target custom 3D head model. We use MeshMixer to select the relevant region of the morphed head model, uniformly thicken the part and merge to the existing respirator model for maximized fitness.

2.4. Multimaterial 3D printing

3D printed respirators and molds are enabled by a high-resolution and multi-material 3D printer Object 260 made by Stratasys (Fig. 1b), which allows us to print complex geometries with 20 μm in resolution. The materials we used for printing is ABS for the respirator cap model in connection to other medical equipment, which has $\rho = 1175$ mg/cm^3, $E = 1.11$ GPa, and $\sigma = 57.9$ MPa corresponding to the density, Young's modulus, and tensile strength of the bulk material properties, as well as Agilus30Black for the flexible respirator body, which has $\rho = 1175$ mg/cm^3, $E = 0.18$ MPa and $\sigma = 0.42$ MPa.

2.5. Mold design for silicone casting

We take the geometric features of a standard type IV dog bone sample to design and build a two-piece mold for casting silicone. The mold was produced with the 3D printer. The upper part is designed with two 5 mm holes to connect to coffee straws to get rid of air bubbles and extra material during model casting.

2.6. Polymer resins for casting respirator

The primary materials used to casting the respirator are silicone rubber and polyurethane, as they are generally available on the market from multiple providers. The general procedure of casting includes 1). Mix material A/B according to the mixture ratio as designed and evenly. 2). Put the mixture into the vacuum chamber and activate the pump to eliminate air bubbles. 3). After eliminating the bubbles, spray the release agent (Sprayway NO. 946 Silicone Spray ("SW946 Silicone Spray," n.d.), alternative mold release includes Vaseline) to the bottom and top part of the mold and then put the mixture into the mold and cover the top part. (act fast since some materials have limited pour time) 4). Close the mold and put the weight on the top part to squeeze out the extra material. 5). Wait different demold times for the material to fully cure, take the sample out, and clean. Table 1 summarizes the mixture ratio, pour time, and demold time of different materials for making the respirator. Silicone 1–4 are obtained from Polytek with the product number of PlatSil® Gel-10, PlatSil® 73-20, PlatSil® 73-45, and PlatSil® 73-60, respectively (Polytek, n.d.). Polyurethane is from Thermosetsolutions with a product number of HSA340 (Solutions, n.d.).

Table 1
Summary of the mixture ratio, pour time, and demold time of different candidate polymer resins with their mechanics tested (Fig. 3) for making the respirators.

Type of Material	Mixture Ratio		Pour Time (Minutes)	Demold Time (Hours)
	A	B		
Silicone 1	1	1	6	0.5
Silicone 2	1	1	5	1
Silicone 3	1	10	40	16
Silicone 4	1	10	45	16
Polyurethane	1	1	7	2–3

2.7. The casting of the respirator

The material that used to make the respirator is the PlatSil® Gel-10. The central part of the respirator, which is made by silicone gels, needs to mix two different kinds of gels. The mix ratio by weight between resin A to resin B is 1:1. We measure 55–60 g A into 55–60 g B with a scale. The mold is designed with 4 holes with coffee straws on the top of the mold. When pressuring the top of the mold, the residue air and excess gel will flow upward along with the straw. Before pouring, spray the release agent inside the mold for easy mold release. After 30–40 min after pouring, the gel is completely set. Take off the top part of the mold by rotating the 6 screws on the top. And then take off the respirator and clean the mold.

2.8. Mechanical testing of the material samples

Using the Instron 5966 machine, we test all the material samples to get their stress-strain curve. We use the 10 KN static load cell with 1 KN pneumatic grips to hold the dog-bone sample for testing. The pressure to drive the pneumatic grips for holding is set to 90 psi. We measure the initial sample length as the distance between the edge of the two grips as L_0 and zero the force and displacement before the test. A pin fixes the lower grips during the test, and the upper grips move at a constant displacement speed of $v = 20$ mm/min. The traveling distance of the upper grips is given by $d = vt$ at any time t after the test starts, and the engineering strain is defined by $\varepsilon = \frac{d}{L_0}$. The load cell records the loading force f and computes the engineering stress with $\sigma = \frac{f}{A_0}$, where A_0 is the initial cross-section area of the uniform testing region of the dog-bone sample. The test automatically stops when the sample is broken. The software with the Instron machine returns the $\sigma - \varepsilon$ curve as well as Young's modulus, yield stress, and breaking strain during the test.

3. Results and discussion

3.1. 3D printing of sterilizable respirator and airtight testing

One way to reduce the usage of polypropylene is to use a sterilizable material to make the regions of the respirator with the main function of giving structural support. These regions can be fully closed to prevent infectious materials from entering, leaving the rest of the area covered by the non-woven fabric or by connecting to other respiratory devices. Fig. 1b shows the fast prototype of such a respirator with a polyjet multi-material 3D printer (Grezzana et al., 2020; Qin et al., 2017; Xiang Gu et al., n.d.). The 3D model was modified based on an open-source stereolithography file ("MY FACE MASK: 3D printed face Mask with a replaceable filter," n.d.), which has a thickness of ~0.5 mm, and the overall shape was designed based on a 3D scanning of a model face. The advantage of this polyjet multi-material 3D printer is the high resolution and the UV curing printing process that prevent generating small gaps and defects.

After printing, the respirator was worn with elastic bands and we tested the airtight of the device by using a simple device composed of an Arduino chip and a CO_2 sensor (Fig. 1c and d). Because the respirator

and human face will not permanently adhere, gaps allow air leakage and infectious materials can occur during either the inhale or exhale process. With the existence of filtering material, the pressure within the respirator during inhaling can be smaller than the atmosphere and thus generate a larger pressing force against the human face that minimizes the respirator gaps. Thus, we mainly focus on detecting the gap and associated air leak during the exhale. We use a CO_2 sensor here based on the fact that the CO_2 content during the exhale process (38,000 ppm) (Siobal, 2016) is much higher than the content in the natural environment (409 ppm) (Lindsey, 2020; Lüthi et al., 2008), making it possible to detect the location of the leak by recording the CO_2 content around the respirator during its usage. It is shown that although the major body of the respirator has no air leak (Fig. 1e), as the CO_2 content at most places of the respirator edge is measured to be ~500 ppm (same as the overall indoor CO_2 content), the region between the mask and the upper side of the nose is recorded as high as 1500 ppm, suggesting the local leakage.

This situation cannot be improved much by simply tightening the elastic band, reducing or increasing the overall mask size, or even changing the mask material from rigid plastic to rubber-like material, as they all lead to a similar situation. Moreover, wearing the hard plastic is rather uncomfortable, and the entire printing process takes more than 20 h because of the slow printing speed, motivating us to explore ways to improve the model and producing method.
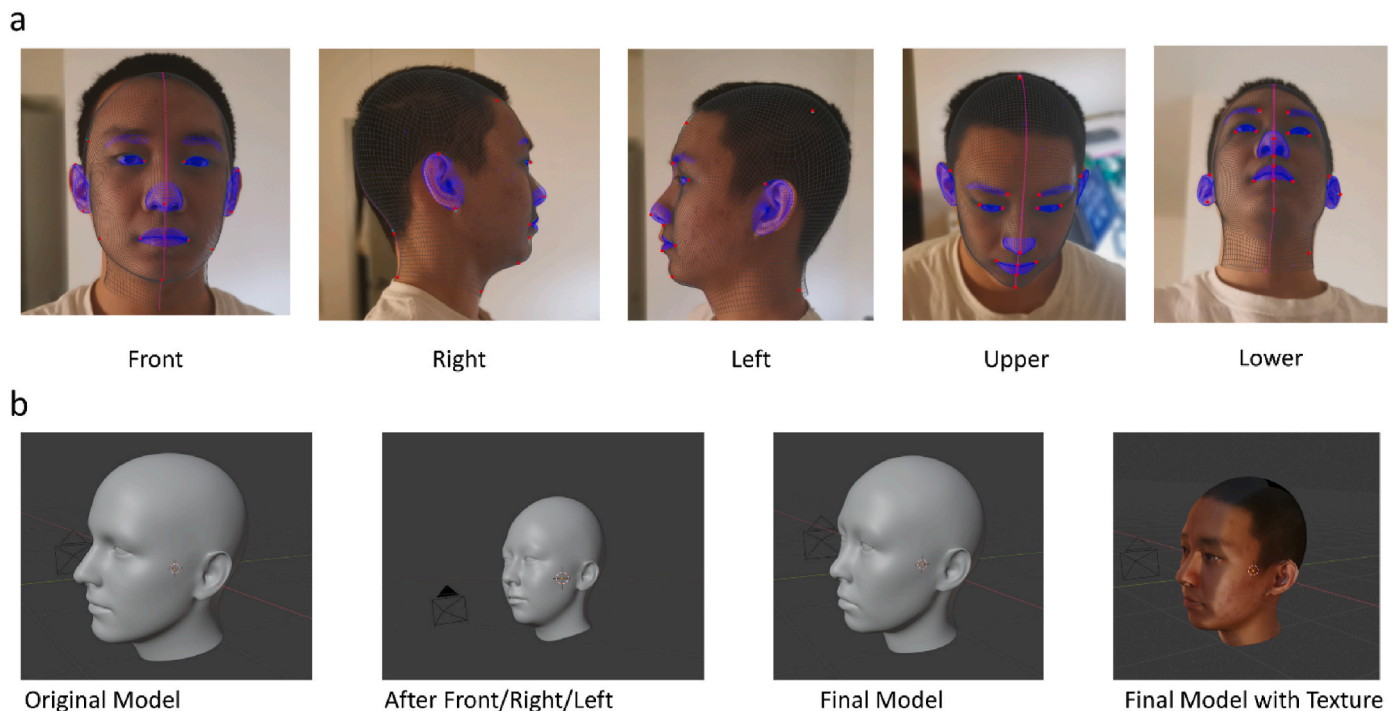
3.2. Customized 3D face profile by morphing

We improve the design of the respirator by altering its shape to maximize its fitness to a specific person's facial profile. There are several hand-hold 3D scanning devices available and most of them require specialized software and hardware to work (Su et al., 2018; Tong et al., 2012). They work by using the sheet laser to project a line of light onto the surface while two sensor cameras continuously record the changing distance and shape of the laser line in three-dimensional space as it sweeps along the object. These methods are limited by the availability of the equipment and the consumption of processing time and

computational resource, as the 3D modeling always starts from scratch. To reduce the barrier and make it possible for everyone to get their respirator, we use an image-based method. Here, we used the Blender package (v2.8.2) to accurately generate the 3D customized face profile (Fig. 2). The add-on tool for Blender makes it convenient to morph an arbitrary shell surface to the face profile according to a couple of photographs (Fig. 2a), which any phone camera can take. In the actual application, two photos are the minimum number of the photo needed to generate the head model, which is one photo from the front and one from the side, as well as some guidance to the tool to point out the location of the reference points on the photo (e.g., eyes, forehead, mouth, nose, etc) will be necessary to generate a 3D shell model according to the customized face profile (Fig. 2b). There can be more photos added throughout the process and the accuracy of the head model will be increased by adding more feature points through these additional photos.

3.3. Use strong, durable silicone for respirator material

Silicones are widely used in engineering applications (e.g., sealants, adhesives, lubricants, medicine, cooking utensils, and thermal and electrical insulation). Such rubber-like materials have the advantage of mechanical strength and thermal stability (Polytek, n.d.). Instead of using 3D printing material, which is slow and subject to limited material types, we choose to use silicone to make the masks (Table 1). We 3D print the molds of the dog-bone sample and use them to cast and prepare the mechanical samples for testing different silicone gels (Polytek, n.d.). The loading curves (Fig. 3a–e with their main mechanical features summarized in Table 2) show that all silicone materials are strain stiffening, in contrast to the strain-softening polyurethane (as another resin material for mold casting) (Solutions, n.d.), suggesting that these materials are flexible at relaxation and small deformation but becomes more difficult to deform for large deformation. This overall strain-stiffening feature is similar to the cytoskeleton and many biological tissues including pigskin (Fig. 3f), making them more compatible

a

Front   Right   Left   Upper   Lower

b

Original Model   After Front/Right/Left   Final Model   Final Model with Texture

Fig. 2. Using simple photos to customize the face profile 3D model for accurate mask design. a. Different featuring points are selected from the photo to recognize their 3D coordinates for face morphing. **b.** illustrate of how the model profile is edited from the original model after receiving information from different photos.
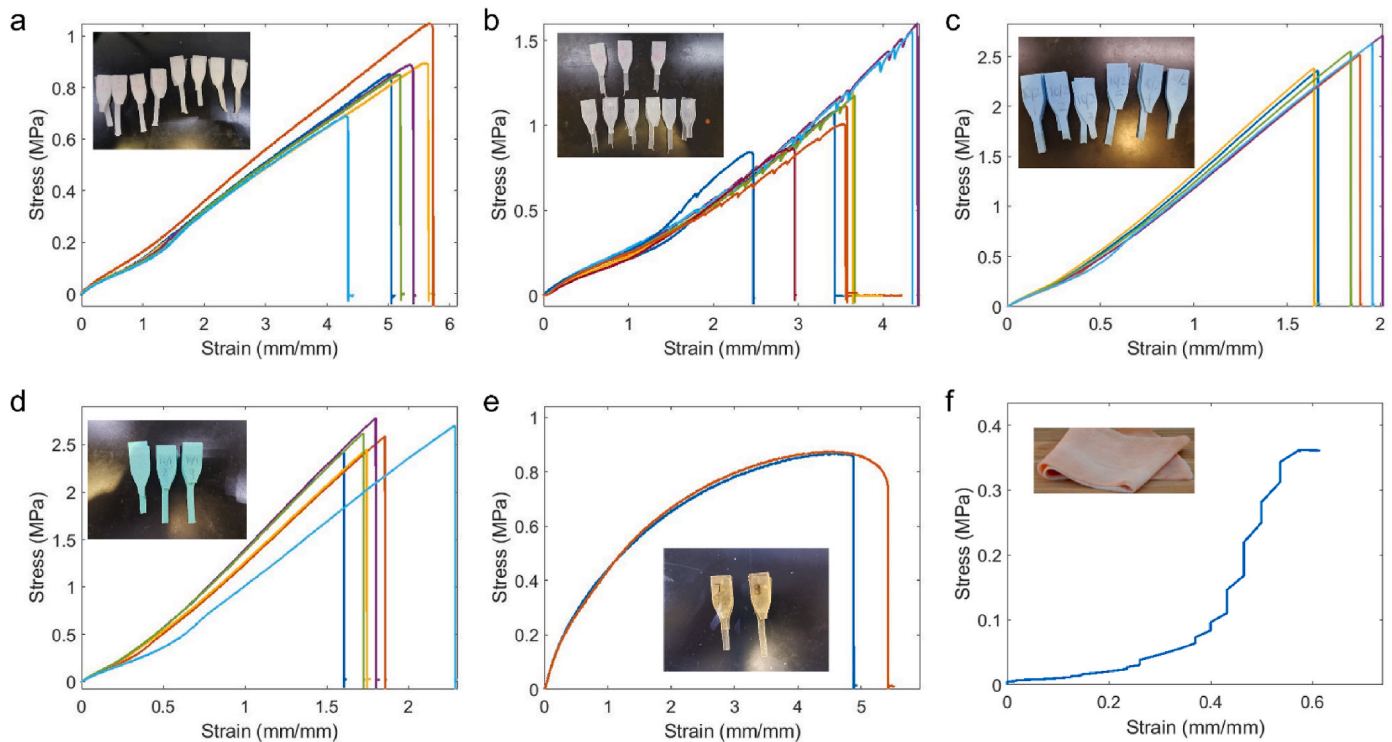
Fig. 3. Stress-strain curve of different polymer materials in comparison to natural material. (**a-d**) for 4 different kinds of silicone rubbers (Polytek, n.d.) and (**e**) for a polyurethane material (Solutions, n.d.). We tested different materials a few times to reduce the error from preparing the sample. **f.** the stress-strain curve of pigskin in a tensile test. It is shown that the overall strain stiffening behavior of the silicone rubbers agrees with that of natural skin and is thus more mechanically compatible than other strain softening polymers. Different line colors in each panel simply mean different repeats of the mechanical test with the same testing parameters. The statistical results of the mechanical properties of the materials are summarized in Table 2. (For interpretation of the references to color in this figure legend, the reader is referred to the Web version of this article.)

Table 2

Summary of the mechanical features including Young's modulus (E), yield strength (σ_Y), ultimate strength (σ_U), and corresponding strain (ε_B) of the polymer materials that have been tested in tensile loading tests.

	E (MPa)	σ_Y (MPa)	σ_U (MPa)	ε_B
Silicone 1	0.28 ± 0.04	0.87 ± 0.08	0.87 ± 0.08	5.43 ± 0.14
Silicone 2	0.79 ± 0.12	1.13 ± 0.19	1.13 ± 0.19	3.54 ± 0.25
Silicone 3	0.91 ± 0.09	2.46 ± 0.04	2.46 ± 0.04	1.8 ± 0.11
Silicone 4	0.98 ± 0.02	2.52 ± 0.07	2.52 ± 0.07	1.85 ± 0.17
Polyurethane	0.62 ± 0.01	0.00124 ± 0.00013	0.78 ± 0.04	5.20 ± 0.20

with the face than other 3D printed plastics. It is noted that the loading curve of the pigskin is not very smooth because the sample slips from the grips during test and we numerical remove the effect of slipping from the strain (Ling et al., 2016). We want to emphasize that this loading test on the pigskin has not reach the rupture strength but it can clearly show the strain stiffening behavior. It is also found that most of the silicone materials have the strength of the same order of magnitude (break at few MPa) while one of them provides the largest extensibility (breaking strain as 5.43 ± 0.14) and lowest Young's modulus (0.28 ± 0.04 MPa), making it more suitable for making the wearable device.

Silicone is a cause of allergic dermatitis, but allergies caused by it are very rare. The major allergen may be a by-product from the manufacturing process, rather than the silicone itself (Prasad and Reeder, 2021). At the same time, only a small area of the silicone will contact the human's face, so the size of contact has been limited to a small region of a ring shape (Fig. 4a). Thus, the device made of silicone is appliable to most people. Meanwhile, the silicone respirator studied in this paper is in analogy to an Elastomeric Half Mask Respirator (EHMR), which has shown more advantage in safety and fitness than N95 facemasks (Barros et al., 2021). Moreover, the oxygen permeability is

important for the gas exchange of the skin cells. It is known that silicone has a much higher (25 time) permeability to oxygen than natural rubber and the permeability increase with temperature (Zhang and Cloud, 2006), which is another reason to use silicone of the respirator. Other allergic test with skin will be necessary before the application of the respirator and that will be included in the future study.

3.4. Customized design of respirator and scalable manufacturing

Instead of directly printing the respirators, we use the high-precision 3D printer to prepare the molds for casting the respirators for efficiency and scalability. The geometry of the 3D model is modified by incorporating a sealant ribbon, as the grey part of Fig. 4a with its geometry cut from the face profile and uniformly extruded, to improve the airtight performance. This entire modified mask model is then used to generate the negative and positive molds for casting silicone, which is composed of 4 pieces as shown in Fig. 4b to make it easy to take off the mask after curing. We use the simple vacuum chamber to remove the air bubbles after mixing the silicone materials and use weight and clamps to push the 4 pieces together after pouring the silicone (Fig. 4b–d). Instead of using more than 20 h in printing and cleaning the mask, this process generally takes less than 30 min, including material preparation and mold cleaning, making it much more scalable.

Wearing the mask is easy as the shape fully adapts to the individual face profile. It does not need to adjust the piece of metal over the nose and dramatically helps to reduce the common mistakes in mask-wearing, as the place where the mask best fits the face provides maximum protection. It is made of silicone makes it more comfortable to wear than hard plastic. Using the CO_2 sensor, we test the airtight of the new respirator by blocking its front with both a regular paper towel and a piece of surgery mask (Fig. 4e), the testing results, as shown in Fig. 4f
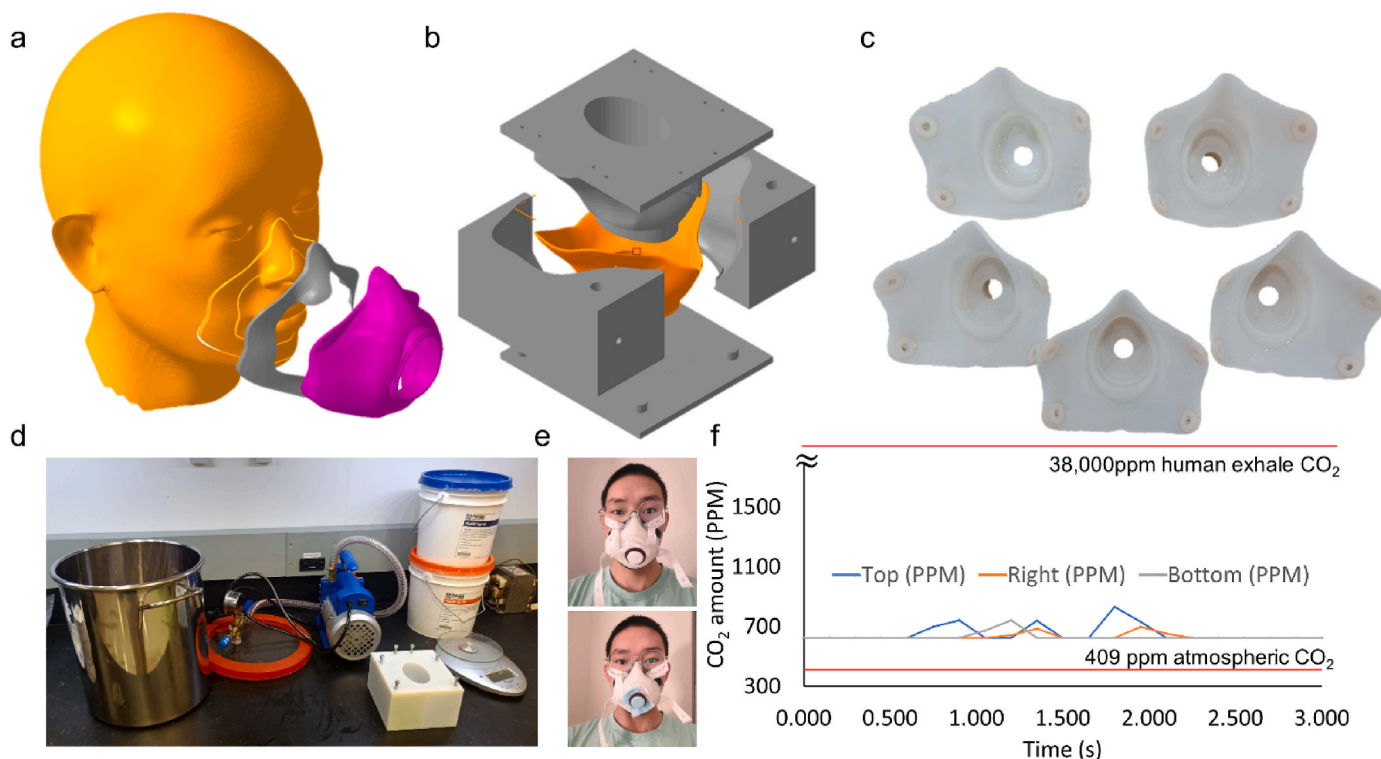
Fig. 4. Design and production of the customized respirator. a. 3D model of the respirator modified according to the customized face profile (orange) for large fitness. **b.** the 4-pieces mold (grey) used to cast and make the silicone respirator (orange). **c.** The silicone respirators are made from mold. **d.** simple devices (vacuum chamber, pump, mold, silicone gels) are used to make the mask. **e.** testing of the mask for airtight by blocking the front with a piece of paper towel (upper) and surgery respirator (lower). This is to qualitatively mimic the effect of the filter of the respirator in blocking the airflow, in order to test the breathability and air tightness of the respirator against the face. **f.** the CO_2 was recorded during normal breathing at different positions. The low CO_2 magnitude suggests airtight at any place around the mask edge. (For interpretation of the references to color in this figure legend, the reader is referred to the Web version of this article.)

for the surgery mask, for example, both suggest that all the periphery regions of the mask (i.e., top, bottom, right) are adequately sealed as the CO_2 level is much lower than that in the exhaled air during the normal breathing.

3.5. Respirator sanitizing

Unlike the reusable respirators currently on the market, the silicone respirators we designed do not need to use a specific disinfectant or disinfectant wipes for treatment. Such a disinfection procedure also increases the waste of materials. Silicone respirators can be directly put into boiling water or 75% alcohol for immersion disinfection. Please note that this article does not study the sterilization function of disinfection time against viruses or air pollutants but only studies the effect of disinfection time and method on the durability of the respirator body.

We immersed the same batch of silica gel dog bone samples in the same volume of 100 °C boiling water and 75% alcohol for different periods (Fig. 5 and Table 3). By doing the tensile test of all the samples, the breaking strain and Young's Modulus remain the same compared to the dog-bone sample without sanitizing. The variance in the loading curve (Fig. 5a and b) mainly comes from the imperfections introduced during the material pouring and sample preparation while the mean values of the mechanical properties after repeating test are very consistent with the results without treatments (Table 3). According to US Centers for Disease Control and Prevention (CDC, ("Making Water Safe in an Emergency," n.d.)), a minute of boiling water is sufficient for sanitizing. We have kept the sample in the boiling water for up to 8 h, which is equivalent to 480 times of sanitizing. To understand the behavior of the silicone material in cyclic loading, we apply a cyclic loading test to the material sample for 100 cycles (Fig. 5c). It is noted that for a large upper limit strain ($\varepsilon = 2.0$), the silicone loses its strength

quickly only in the first 20 cycles, mainly because of the local material failure at the holding grips due to the large shear stress in biaxial loading (inserted image of the sample in Fig. 5c). However, the strength lost becomes very small during the following cycles (inserted plot in Fig. 5c). By linear fitting the peak force as a function of the loading cycle, we can predict that it would take at least 310 cycles before reaching half of the strength. Moreover, by using Scanning Electron Microscope (SEM) we do not observe any structural defects that is caused by the boiling water or alcohol (Fig. 5d–f). The test result, combined with the boiling water and alcohol test, make us believe that the material can be subjected to at least a few hundreds of cycles of sanitizing and loading. The test results show that the respirator body's durability will not be affected after disinfection with a different method, so the respirator can be reused and disinfected with a simple ingredient.

4. Conclusion

Here, we study the ways to design and manufacture respirators that can be re-sterilized for most of the respirator body that maximize personal protection (Akber Abbasi et al., 2020; Rubio-Romero et al., 2020; Sangkham, 2020; Selvaranjan et al., 2021). We find the shape is crucial to make it comfortable for wearing and effective protection and should fully adapt to individual face profiles. We find an effective solution of using single photos to build an accurate 3D face model to design the mask geometry. We compare different materials with mechanical tests and identify the silicone material as effective in providing flexibility, strength, and thermal stability in making the mask. As well as the material with sanitizing treatment. As the respirator is fully customized, we use a high-precision 3D printer to produce the molds that are used to cast and massively produce the silicone masks. We test the respirator's performance and find that it is comfortable to wear and provides airtight in
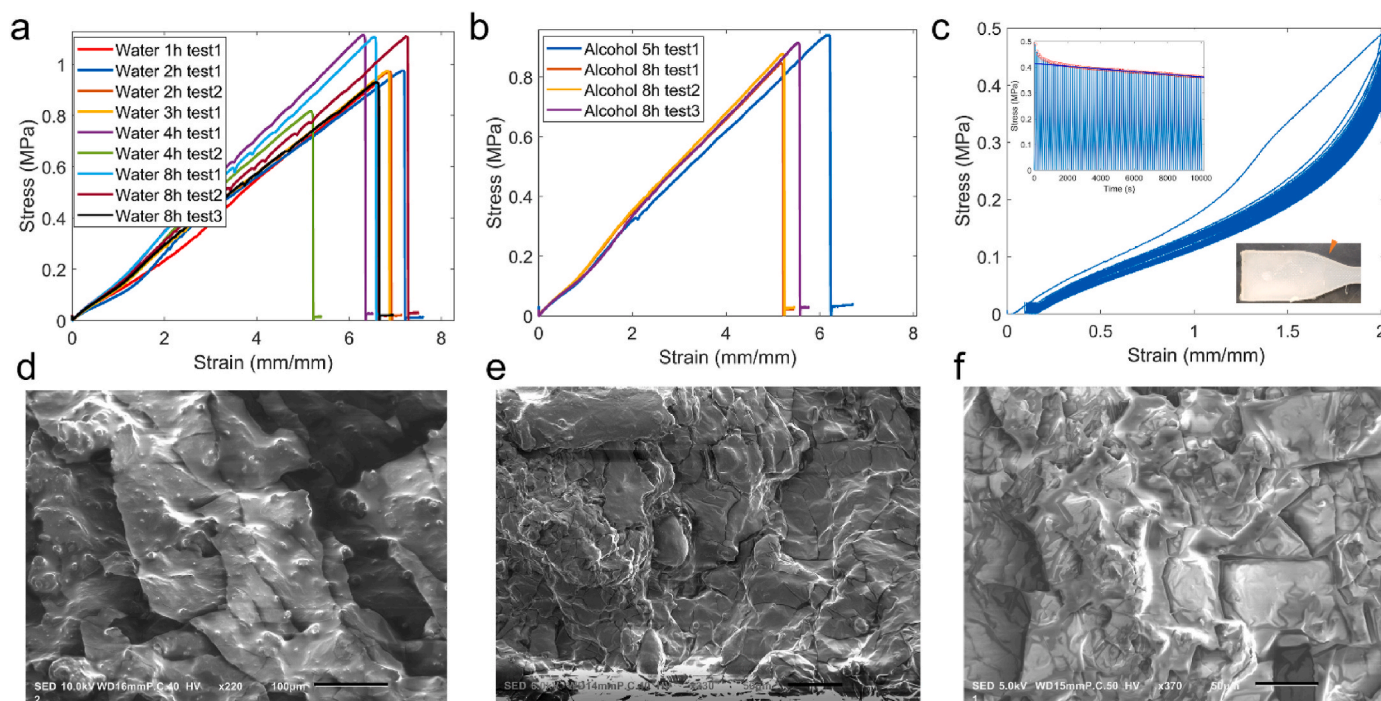
Fig. 5. Stress-strain curve and SEM images of Silicone 1 Material in different sanitizing treatment times. a. Sanitizing in boiling water for 1, 2, 3, 4, and 8 h, respectively. **b.** Sanitizing in Alcohol for 5 and 8 h, respectively. We tested different materials a few times to reduce the error from preparing the sample and the statistical results of the mechanical properties of the materials are summarized in Table 3 **c.** the stress-strain curve of Silicone 1 sample under 100 loading-unloading cycles with a constant speed of 100 mm/min and the upper strain of 2.0. The inserted plot gives the stress history as a function of the time and shows how the peak stress decay as the number of loading cycles. SEM images of **d.** original Silicone 1 dogbone sample (without treatment, scale bar: 100 μm) **e.** with treatment in boil water for 4 h (scale bar: 50 μm) and **f.** with treatment in Alcohol for 8 h (scale bar: 50 μm). By comparing the SEM images (**d, e, f,** and many others not shown), we do not find any significant difference in the microstructure of the silicone surface after the treatment.

Table 3

Summary of the mechanical features including Young's modulus (E), yield strength (σ_Y), ultimate strength (σ_U), and corresponding strain (ε_B) of the Silicone 1 after certain sanitization treatment (boiled water or 75% alcohol) conditions.

Condition	E (MPa)	σ_Y (MPa)	σ_U (MPa)	ε_B
Boiled Water (1h)	0.33	0.92	0.92	6.31
Boiled Water (2h)	0.32 ± 0.03	0.97 ± 0.03	0.97 ± 0.03	6.90 ± 0.19
Boiled Water (3h)	0.35	1.0	1.0	6.8
Boiled Water (4h)	0.40 ± 0.05	0.90 ± 0.08	0.90 ± 0.08	5.73 ± 0.20
Boiled Water (8h)	0.36 ± 0.10	1.03 ± 0.15	1.03 ± 0.15	6.77 ± 0.21
75% Alcohol (5h)	0.27 ± 0.05	0.95 ± 0.12	0.95 ± 0.12	6.23 ± 0.26
75% Alcohol (8h)	0.25 ± 0.02	0.87 ± 0.04	0.87 ± 0.04	5.27 ± 0.31

all the periphery directly during the entire breathing process.

The method we proposed in this study can lead to flexible respirators that can provide the wearers more comfort. They are easy to carry and store, which is essential in manufacturing, mining, and other intense work. These designs are reusable and easy to sanitize without losing its mechanical strength. The respirators are fully reusable, and their broad usage may help to reduce the negative impact to the environment waste of single-use respirators by only changing its filter.

One method to make the design process more automatic and suitable for large-scale production is to categorize further different face profiles (Richmond et al., 2018; Valentine et al., 2004). Instead of building the customized face model for each individual, which requires an infinite number of molds for production, categorizing all the face profiles into a limited number of standard models will lead to a few molds. For that purpose, we will need to use machine learning to learn from the extensive library of face profiles, categorize them and develop a printed mask model for each category. For customized design, image-based machine learning (Z. Yang et al., 2021) can be used to determine

which category is more suitable for a person quickly and thus help to select the respirator type. Moreover, once massive production of a certain respirator model is necessary, production of metal molds of durability can be done by 3D metal printing via the Selective Laser Melting technique and using rubber-like thermal plastic polymers can further accelerate the filling and demolding process for massive production.

To balance the environmental issue and personal protection during the usage of respirators, one solution is to develop substituting fibrous network material that can provide similar protection but will not generate environmental issues in the long term. Natural materials including chitin, cellulose, hemicellulose, silk, collagen, keratin are found to have forms of various fibrous networks including mycelium (L. Yang et al., 2021), bamboo/wood/cotton fibers (Cui et al., 2021), spider web/cocoon, basement membrane, and hair (Buehler and Yung, 2009) that all have natural functions of filtration but can also be degraded within a more reasonable timeframe than plastics by microorganisms, causing no long-term issue to the environment (Greer and Deshpande, 2019; Grezzana et al., 2020; Jones et al., 2020; Qin and Buehler, 2013; Shah et al., 2016). It is feasible to make fibrous membrane by using these biodegradable materials with an electro/melt spinning method and tailor the membrane into pieces of a desire shape to work as a changeable filter for the respirator. The respirator can connect to different covers as the adaptor to different changeable filtering devices. Since the main body of the respirator can be sanitized and reused, it can significantly reduce the waste generation. However, the chemical and mechanical functions of these degradable materials highly depend on their chemical sequences and molecular structures and thus is crucial to understand their relationship via multiscale modeling, optimize through statistical studies and design the specific process to produce new strong fibrous materials not dissolve and weaken in water (Arbelaiz et al., 2005), while also provide recyclability and environmental safety at the

same time for air filtering.

Notes

The authors declare no competing financial interest.

CRediT authorship contribution statement

Declaration of competing interest

The authors declare that they have no known competing financial interests or personal relationships that could have appeared to influence the work reported in this paper.

Acknowledgments

References

Akber Abbasi, S., Khalil, A.B., Arslan, M., 2020. Extensive use of face masks during COVID-19 pandemic: (micro-)plastic pollution and potential health concerns in the Arabian Peninsula. Saudi J. Biol. Sci. 27, 3181–3186. https://doi.org/10.1016/j.sjbs.2020.09.054.

Arbelaiz, A., Fernández, B., Ramos, J.A., Retegi, A., Llano-Ponte, R., Mondragon, I., 2005. Mechanical properties of short flax fibre bundle/polypropylene composites: influence of matrix/fibre modification, fibre content, water uptake and recycling. Compos. Sci. Technol. 65, 1582–1592. https://doi.org/10.1016/j.compscitech.2005.01.008.

Barros, A.J., Sifri, C.D., Bell, T.D., Eby, J.C., Enfield, K.B., 2021. Effectiveness of elastomeric half-mask respirators vs N95 filtering facepiece respirators during simulated resuscitation: a nonrandomized controlled trial. JAMA Netw. Open 4. https://doi.org/10.1001/jamanetworkopen.2021.1564.

Buehler, M.J., Yung, Y.C., 2009. Deformation and failure of protein materials in physiologically extreme conditions and disease. Nat. Mater. https://doi.org/10.1038/nmat2387.

Canopoli, L., Coulon, F., Wagland, S.T., 2020. Degradation of excavated polyethylene and polypropylene waste from landfill. Sci. Total Environ. 698 https://doi.org/10.1016/j.scitotenv.2019.134125.

Chaib, F., 2020. Shortage of Personal Protective Equipment Endangering Health Workers Worldwide [WWW Document]. WHO News release. URL https://www.who.int/news/item/03-03-2020-shortage-of-personal-protective-equipment-endangering-health-workers-worldwide.

Chellamani, K.P., Veerasubramanian, D., Vignesh Balaji, R.S., 2013. Surgical face masks: manufacturing methods and classification. J. Acad. Ind. Res. 2, 320.

Cui, J., Jiang, M., Nicola, M., Masic, A., Qin, Z., 2021. Multiscale understanding in fracture resistance of bamboo skin. Extrem. Mech. Lett. 49, 101480 https://doi.org/10.1016/j.eml.2021.101480.

Greer, J.R., Deshpande, V.S., 2019. Three-dimensional architected materials and structures: design, fabrication, and mechanical behavior. MRS Bull. 44, 750–757. https://doi.org/10.1557/mrs.2019.232.

Grezzana, G., Loh, H.C., Qin, Z., Buehler, M.J., Masic, A., Libonati, F., 2020. Probing the role of Bone Lamellar patterns through Collagen microarchitecture mapping, numerical modeling, and 3D-printing. Adv. Eng. Mater. 22 https://doi.org/10.1002/adem.202000387.

Jones, M., Mautner, A., Luenco, S., Bismarck, A., John, S., 2020. Engineered mycelium composite construction materials from fungal biorefineries: a critical review. Mater. Des. 187, 108397 https://doi.org/10.1016/j.matdes.2019.108397.

Lindsey, R., 2020. Climate change: atmospheric carbon dioxide. Nature 453, 379–382.

Ling, S.J., Zhang, Q., Kaplan, D.L., Omenetto, F., Buehler, M.J., Qin, Z., 2016. Printing of stretchable silk membranes for strain measurements. Lab Chip 16, 2459–2466. https://doi.org/10.1039/c6lc00519e.

Lüthi, D., Le Floch, M., Bereiter, B., Blunier, T., Barnola, J.M., Siegenthaler, U., Raynaud, D., Jouzel, J., Fischer, H., Kawamura, K., Stocker, T.F., 2008. High-resolution carbon dioxide concentration record 650,000-800,000 years before present. Nature 453, 379–382. https://doi.org/10.1038/nature06949.

Making Water Safe in an Emergency, Making Water Safe in an Emergency [WWW Document], n.d. URL https://www.cdc.gov/healthywater/emergency/making-water-safe.html.

MY FACE MASK: 3D printed face Mask with a replaceable filter [WWW Document], n.d. URL https://www.3dwasp.com/en/3d-printed-mask-from-3d-scanning/.

NIOSH, 1996. NIOSH Guide to the Selection and Use of Particulate Respirators [WWW Document]. NIOSH Publ. number 96101. URL https://www.cdc.gov/niosh/docs/96-101/.

Oladimeji Azeez, T., 2020. Thermoplastic recycling: properties, modifications, and applications. In: Thermosoftening Plastics. https://doi.org/10.5772/intechopen.81614.

Polytek, n.d. PlatSil Silicone Gels Technical Bulletin.

Prasad, A., Reeder, M.J., 2021. Allergic contact dermatitis to silicone in a continuous positive airway pressure mask. Contact Dermatitis 84, 460–462. https://doi.org/10.1111/cod.13759.

Qin, Z., Buehler, M.J., 2013. SPIDER SILK Webs measure up. Nat. Mater. 12, 185–187. https://doi.org/10.1038/Nmat3578.

Qin, Z., Jung, G.S., Kang, M.J., Buehler, M.J., 2017. The mechanics and design of a lightweight three-dimensional graphene assembly. Sci. Adv. 3, e1601536 https://doi.org/10.1126/sciadv.1601536.

Richmond, S., Howe, L.J., Lewis, S., Stergiakouli, E., Zhurov, A., 2018. Facial genetics: a brief overview. Front. Genet. https://doi.org/10.3389/fgene.2018.00462.

Rubio-Romero, J.C., Pardo-Ferreira, M. del C., Torrecilla-García, J.A., Calero-Castro, S., 2020. Disposable masks: disinfection and sterilization for reuse, and non-certified manufacturing, in the face of shortages during the COVID-19 pandemic. Saf. Sci. 129 https://doi.org/10.1016/j.ssci.2020.104830.

Sangkham, S., 2020. Face mask and medical waste disposal during the novel COVID-19 pandemic in Asia. Case Stud. Chem. Environ. Eng. 2, 100052 https://doi.org/10.1016/j.cscee.2020.100052.

Selvaranjan, K., Navaratnam, S., Rajeev, P., Ravintherakumaran, N., 2021. Environmental challenges induced by extensive use of face masks during COVID-19: a review and potential solutions. Environ. Challenges 3, 100039. https://doi.org/10.1016/j.envc.2021.100039.

Shah, A.U.M., Sultan, M.T.H., Jawaid, M., Cardona, F., Talib, A.R.A., 2016. A review on the tensile properties of bamboo fiber reinforced polymer composites. Bioresources 11, 10654–10676. https://doi.org/10.15376/biores.11.4.Shah.

Siobal, M.S., 2016. Monitoring exhaled carbon dioxide. Respir. Care 61, 1397–1416. https://doi.org/10.4187/respcare.04919.

Solutions, T, n.d. HSA 340 - Thermoset Solutions.

Su, I., Qin, Z., Saraceno, T., Krell, A., Mühlethaler, R., Bisshop, A., Buehler, M.J., 2018. Imaging and analysis of a threedimensional spider web architecture. J. R. Soc. Interface 15. https://doi.org/10.1098/rsif.2018.0193.

SW946 Silicone Spray [WWW Document], n.d. URL https://www.spraywayinc.com/sites/all/themes/theme687/techsheets/sw946_techsheet.pdf.

Tong, J., Zhou, J., Liu, L., Pan, Z., Yan, H., 2012. Scanning 3D full human bodies using kinects. IEEE Trans. Visual. Comput. Graph. 18, 643–650. https://doi.org/10.1109/TVCG.2012.56.

Tong, Y., Pan, J., Kucukdeger, E., Johnson, A.L., Marr, L.C., Johnson, B.N., 2021. 3D printed mask frames improve the inward protection efficiency of a cloth mask. ACS ES&T Eng. https://doi.org/10.1021/acsestengg.1c00028.

Valentine, T., Darling, S., Donnelly, M., 2004. Why are average faces attractive? The effect of view and averageness on the attractiveness of female faces. Psychon. Bull. Rev. 11, 482–487. https://doi.org/10.3758/BF03196599.

Xiang, Y., Song, Q., Gu, W., 2020. Decontamination of surgical face masks and N95 respirators by dry heat pasteurization for one hour at 70°C. Am. J. Infect. Control 48, 880–882. https://doi.org/10.1016/j.ajic.2020.05.026.

Xiang Gu, G., Su, I., Sharma, S., Voros, J.L., Qin, Z., Buehler, M.J., n.d. Three-dimensional-printing of bio-inspired composites. J. Biomech. Eng. 138, 21006. https://doi.org/2480954.[pii]10.1115/1.4032423.

Yang, L., Park, D., Qin, Z., 2021. Material function of mycelium-based bio-composite: a review. Front. Mater. https://doi.org/10.3389/fmats.2021.737377.

Yang, Z., Yu, C.-H., Buehler, M.J., 2021. Deep learning model to predict complex stress and strain fields in hierarchical composites. Sci. Adv. 7, eabd7416 https://doi.org/10.1126/sciadv.abd7416.

Zhang, H., Cloud, A., 2006. The permeability characteristics of silicone rubble. In: International SAMPE Technical Conference.